Research Journal of Applied Sciences, Engineering and Technology10(9): 997-1006, 2015
DOI: 10.19026/rjaset.10.1866
ISSN: 2040-7459; e-ISSN: 2040-7467

Submitted: November 27, 2014 Accepted: March 12, 2015 Published: July 25, 2015

Research Article

A Robust Adaptive Sliding Mode Control for PMLSM with Variable Velocity Profile Over Wide Range

Payam Ghaebi Panah, Mohammd Ataei, Behzad Mirzaeian, Arash Kiyoumarsi and Ahmad Shafiei
Department of Electrical Engineering, University of Isfahan, Isfahan, Iran

Abstract: An adaptive robust variable structure speed controller is designed for wide range of desired velocity control of a Permanent Magnet Linear Synchronous Motor (PMLSM). This is performed for comprehensive nonlinear model of PMLSM including non-idealities such as detent force, parameter uncertainty, unpredicted disturbance and nonlinear friction. The proposed method is based on the robust Sliding Mode Control (SMC) in combination with an adaptive strategy for a wide range of velocity. The simulation results are provided for the above mentioned comprehensive model of PMLSM with a variable velocity profile. Moreover, as an evaluation criterion, a Proportional-Integral (PI) controller is designed whose parameters are optimally tuned by the Particle Swarm Optimization (PSO) algorithm for better comparison.

Keywords: Particle swarm optimization, permanent magnet linear synchronous motor, variable structure controller, velocity control

INTRODUCTION

Nowadays, great merits of permanent magnets with reasonable price have appealed engineers to enhance traditional electrical machines. The advent of linear motors is not very recent; however, permanent magnet linear synchronous motors have become the first choice for miscellaneous applications where a linear motion is required. As a matter of fact, PMLSM is capable of providing accurate and rapid linear movement without need to any troublesome mechanical medium. Besides, higher reliability, efficiency and thrust force could make it an unparalleled machine in industrial usages. PMLSMs are used extensively in precision machine tools, semi-conductor manufacture equipment, modern laser cutting, high-speed milling, scanning machines, transportation, conveyor systems, slider door closer, curtain pullers, drop-towers, fast manipulators and super sky scraper elevators (Lee *et al*., 2014).

However, as the dark side, it suffers from a positional dependency in the thrust force that is called detent force. This force arises from the interaction of the permanent magnets and the ferromagnetic core. This undesirable force appears even in the windings without current. Practically, the force ripple of the PMLSM is larger than that of rotary motors because of the finite length of the mover and the wide slot opening. Force ripples may lead to speed oscillations which in turn can deteriorate the performance. The force ripples change periodically as the mover advances during its motion. In fact, all flux linkage harmonics, cogging harmonics and time harmonics are involved in force ripples.

Statistically, most of linear motors are meant to work bi-directionally at relatively low speed. Hence, the designers should pay more attention to different forces and their effects on each part of speed range. Obviously, friction is more nonlinear at low speed and especially around standstill. Furthermore, the performance of PMLSM might greatly affected by the uncertainties, which include not only thrust ripple but also parameter variations and external load disturbances. Altogether, providing a satisfactory movement in PMLSM's slider could be challenging especially in low power machines.

Indeed, there are two different major strategies to reduce the force ripple. The first approach is optimal constructive design of machine; like skewing, shifting of PM position, fractional-slot pitch, non-iron cores, etc. (Hong *et al*., 2013; Shin *et al*., 2014; Kim *et al*., 2014). While, the second approach, by which this study is organized, is to set a control policy to overcome this inefficiency and deteriorating characteristics without any change on machine design parameters. Unfortunately, there are some unpredicted forces and model uncertainties which may deteriorate performance and control scheme. Thus, developing a robust drive which is able to control the velocity of slider under harsh condition is the main object of this research.

Many researchers have employed different control algorithms for PMLSM drives to improve their

Corresponding Author: Payam Ghaebi Panah, Department of Electrical Engineering, University of Isfahan, Isfahan, Iran

performance. For instance, the linearization approach which is not powerful enough due to its dependency on the operating point and also accurate modeling (Seong and Tomizuka, 1996). Another common and straightforward method is state feedback which might be better than classical controllers (Orbak, 2003). On the other hand, some researchers have applied nonlinear control methods to drive systems whose main drawback is to find the corresponding Lyapanov function (Ouassaid and Rkaoui, 2005; Liyi *et al*., 2008). Recently, model reference and sliding mode control are used widely; however, the model reference parameter identification might not be straightforward (Zhao *et al*., 2007).

Sliding mode control can be employed to control position, thrust and velocity (Yang *et al*., 2006; Ghaebi Panah *et al*., 2010; Ghaebi Panah *et al*., 2011a; Rivera *et al*., 2014; Bernardes *et al*., 2014). Besides, other heuristic approaches are adopted such as brain emotional learning based intelligent controller and radial basis function (Ghaebi Panah *et al*., 2011b; Lin *et al*., 2010). In most of researches the linear and simplified model of PMLSM and friction is utilized.

In this study an adaptive robust sliding mode controller is proposed for a wide velocity range. Not only nonlinear model of friction is considered but also uncertainty on parameters has been taken into account. The designed controller has two important advantages: insensitivity to model parameter variation and external disturbances and also satisfying performance in wide range of reference speed. In order to overcome the undesirable chattering phenomenon, which causes high frequency switching on control signal, the controller is enhanced by saturation function instead of sign function.

METHODOLOGY

Modeling: PMLSM is a nonlinear system and its mathematical model is difficult to derive completely. There are famous models briefly presented in this section. As an intuitive approach, the description of PMLSM by electrical relations in the form of an equivalent circuit was proposed; however, it is not widespread and practical (Lin *et al*., 2011). Another model is based on Causal Ordering Graph (COG), which precisely illustrates the interactions between the fluxes and the currents of PMLSM but it is not still straightforward (Jia *et al*., 2003). In fact, the most popular model of PMLSM is based on the synchronous rotating reference frame as follows. However, there are a few assumptions in the process of mathematical modeling foundation. For instance, the iron core saturation is neglected and the losses of eddy currents and hysteresis are not taken into account. Moreover, the mover has not any damper windings. Conductivity of PM material is also zero and induced electromotive force in phase winding is sinusoidal. Thus, the equations of voltage and linkage flux under the d-q rotating coordinate can be written as follows:

$$v_d = R_1 I_{ad} + d\Psi_d / dt - \omega\Psi_q \tag{1}$$

$$v_q = R_1 I_{aq} + d\Psi_q / dt + \omega\Psi_d \tag{2}$$

$$v_f = R_f I_f + d\Psi_f / dt \tag{3}$$

The linkage fluxes are defined as Eq. (4)-(6):

$$\begin{aligned}\Psi_d &= (L_{ad} + L_1) i_{ad} + L_{aq} i_D + \Psi_f \\ &= L_{sd} i_{ad} + L_{ad} i_D + \Psi_f\end{aligned} \tag{4}$$

$$\begin{aligned}\Psi_q &= (L_{aq} + L_1) i_{aq} + L_{aq} i_Q \\ &= L_{sq} i_{aq} + L_{ad} i_Q + \Psi_f\end{aligned} \tag{5}$$

$$\Psi_f = L_{fd} I_f \tag{6}$$

where, v_d, v_q, i_{ad} and i_{aq} are the voltages and currents in mover frame, Ψ_f is the maximum flux produced by the permanent magnet per phase, R_1 is the winding resistance of armature, L_{ad} and L_{aq} are self-inductances, $\omega = \pi v_s/\tau$ is the mover electrical speed, τ is the pole pitch and v_s is the synchronous linear velocity.

Considering the above mentioned assumptions, Eq. (1) and (2) are simplified:

$$v_d = R_1 i_{ad} + L_{sd}\, di_{ad}/dt - \omega L_{sq} i_{aq} \tag{7}$$

$$v_q = R_1 i_{aq} + L_{sq}\, di_{aq}/dt + \omega L_{sd} i_{ad} + \omega\Psi_f \tag{8}$$

Therefore, the electromagnetic power for a three-phase machine can be extracted:

$$\begin{aligned}P_{elm} &= (3\pi v_s/2\tau)[\Psi_d i_{aq} - \Psi_q i_{ad}] \\ &= (3\pi v_s/2\tau)[\Psi_f i_{aq} + (L_{sd} - L_{sq}) i_{ad} i_{aq}]\end{aligned} \tag{9}$$

The electromagnetic thrust of a three phase PMLSM with pole pairs is defined as follows:

$$\begin{aligned}F_{dx} &= p(P_{elm}/v_s) \\ &= (3\pi p/2\tau)[\psi_f i_{aq} + (L_{sd} - L_{sq}) i_{aq} i_{ad}]\end{aligned} \tag{10}$$

If $L_{sd} = L_{sq}$ the electromagnetic thrust is as (11):

$$F_{dx} = p(P_{elm}/v_s) = (3\pi p/2\tau)\Psi_f i_{aq} \tag{11}$$

The motion equation of PMLSM is described as follows:

$$dv_s/dt = [F_{dx} - f_L - F_{fric}]/M \quad (12)$$

where,

f_L = The external load
M = The mover mass
F_{fric} = Nonlinear friction force that will be explained below

Since in this study field oriented control method is adopted for a surface mounted PMLSM ($L_d = L_q$), time harmonics and reluctance forces are neglected and the reference current of d-axis is equal to zero ($i_d = 0$) (Van Den Braembussche *et al*., 1996). Regarding the type of PMLSM which is a fractional-slot pitch, amplitude of back EMF harmonics can be diminished and therefore the effect of flux distortion is neglected. Thus, the most effective force in the thrust ripple is detent force. Indeed, the detent force has to be taken into account to make simulation closer to the real PMLSM. As a matter of fact, remarkable portion of publications are allotted to machine structure optimization in order to reduce the ripple force and subsequently to ameliorate the performance (Hwang *et al*., 2012; Tavana *et al*., 2012). However, this study does not focus on the analysis of motor structure, in the light of formerly done finite element analyses, the detent force can be approximated to a sinusoidal wave and proportional to the position of mover. Amplitude of detent force is normally about 1-2%, but in the worst case and fully pessimistic view, it is assumed 5% here (Inoue and Sato, 2000; Lu and Chang, 2009). The following equations are achieved using state variables:

$$\begin{bmatrix} dI_d/dt \\ dI_q/dt \\ dv/dt \end{bmatrix} = \begin{bmatrix} -R.I_d/L_d + L_q.\pi.v.I_q/(L_d.\tau) + V_d/L_d \\ -R.I_q/L_q - L_d.\pi.v.I_d/(L_q.\tau) - \pi.\lambda_{PM}.v/(L_q.\tau) + V_q/L_q \\ \frac{3\pi.\lambda_{PM}.I_q}{2\tau.M} + \frac{3\pi.I_d.I_q.(L_d - L_q)}{2\tau.M} - \frac{D.v}{M} - \frac{(F_L + F_d)}{M} \end{bmatrix} \quad (13)$$

where, F_d stands for unpredicted forces which are not modeled formerly. These forces can be brought about by wind friction, linear bearings, asymmetrical armature, improper installation, etc.

As mentioned earlier, since d and q axes inductances are the same, equations can be simplified as Eq. (14). Noticeable point is that due to neglecting of dampers, the inductance in Eq. (14) is the total value observed in the direct path. It should be noted that inductance value is smaller than other coefficients in Eq. (14). Hence, nonlinear terms are diminished and the equations are roughly linear:

$$\begin{bmatrix} dI_d/dt \\ dI_q/dt \\ dv/dt \end{bmatrix} = \begin{bmatrix} -R.I_d/L + \pi.v.I_q/\tau + V_d/L \\ -R.I_q/L - \pi.v.I_d/\tau - \pi.\lambda_{PM}.v/L.\tau + V_q/L \\ \frac{3\pi.\lambda_{PM}.I_q}{2\tau.M} - \frac{D.v}{M} - \frac{(F_L + F_d)}{M} \end{bmatrix} \quad (14)$$

where,

$$L = L_{m\sigma} + L_{md} = L_{m\sigma} + L_{mq}$$

Friction force: Since linear motors operate in the range which includes low and zero velocities, the linear and simplified friction model cannot be valid anymore. Behavior of friction force around zero velocity is completely nonlinear and more careful modeling is required. Therefore, in this study special attention is paid to the friction force. As an important physical phenomenon, friction is intensively researched by experiments, modeling and simulation studies. There are four regimes of lubrication for lubricated metallic surfaces in contact: static friction (pre-sliding), boundary lubrication, partial fluid lubrication and full fluid lubrication (Xie, 2008).

In the pre-sliding regime, the asperity junctions deform elastically. Once the tangential force exceeds a certain threshold, referred to as the static friction value, the junctions will break, causing sliding to start; the transition from pre-sliding to sliding is called breakaway. It is noted in tribology literature that static friction level can be a function of dwell time which is the duration that the surfaces are at rest before sliding occurs.

In the boundary lubrication regime, sliding occurs at a very low velocity. Though it is not always true, the friction in this regime is often assumed to be less than that found in fluid lubrication cases. In the partial fluid lubrication regime, the film is not thick enough to completely separate the two surfaces and the contacts at some asperities still affect the friction force. As partial fluid lubrication increases, solid to solid contact between the boundary layers decreases. It may result in the reduction of friction force with increasing velocity. This regime is the most difficult one to model. Furthermore, there is a phase lag between the change in friction and the changes in velocity or load conditions; referred to as frictional memory, this phase lag may be in the order of milliseconds to seconds.

When sliding velocity reaches a certain level, a continuous fluid film is formed which completely separates the two surfaces. In this regime, referred to as full fluid lubrication, the viscosity of the lubricant is dominant on the friction force.

Friction properties can be classified into two categories: static characteristics, which include the kinetic and viscous force and the Stribeck effect; and dynamic characteristics, which comprise pre-sliding

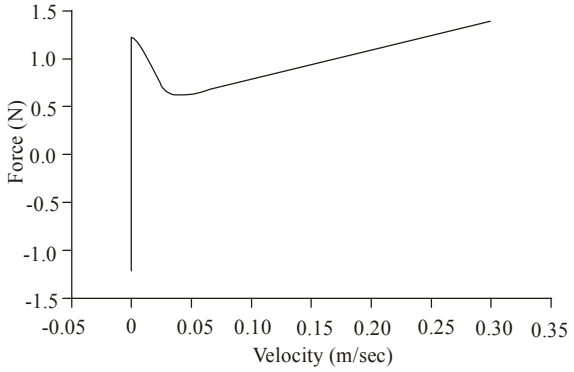

Fig. 1: Friction force

displacement, varying breakaway force, Dahl effect and a frictional lag.

To interpret those observed friction properties, many models are proposed. All of the existing models can be boiled down to static and dynamic models that try to explain the observed friction characteristics. The friction force can be formulated as Eq. (15). Notice that all parameters of the following equation are time varying. All in all, the assumed friction force in this study is depicted in Fig. 1:

$$f(v) = F_c.sign(v) + D.v + (F_s - F_c).\exp(-(v/\upsilon_s)^2).sign(v) \quad (15)$$

where,

υ_s = Stribeck velocity
F_c = Coulomb friction
F_s = Stiction friction
D = Viscous coefficient

Sliding mode controller design: Linear motors are often exposed to external disturbances such as friction force, ripple and load change. Due to lack of interface devices, tracking of reference velocity is heavily affected by external disturbances and model parameter uncertainties (Kung, 2008). Assuming some considerations, the dynamic equation of PMLSM at nominal operating conditions, excluding the external disturbances, can be achieved:

$$\dot{v}.\overline{M}/\overline{K}_F + v.\overline{D}/\overline{K}_F = i_q^* \quad (16)$$

If external disturbances and parameter changes be added to Eq. (16), the following equation is achieved:

$$\dot{v} = (K_F/M)i_q^* - (F_L + f(v) + F_d)/M = f + B_m.U_v + g \quad (17)$$

where, $K_F = 3\pi.p.\lambda_{PM}/(2\tau)$ is thrust coefficient, $U_v = i^*_q$ is reference current of q-axis, $f = -f(v)/M$ is nonlinear friction force, $B_m = K_F/M > 0$ is coefficient of reference current and $g = -(F_L + f(v) + F_d)/M$ is total external force.

The schematic diagram of the velocity control is shown in Fig. 2. Both machine parameter uncertainties and external disturbances are assumed to be bounded by known limit values ($|g| \le G^u$, $B_L \le B_m$ and $|f| \le F^U$; where F^U is a known continuous function, G^U and B_L are known constants regarded to range of uncertainties).

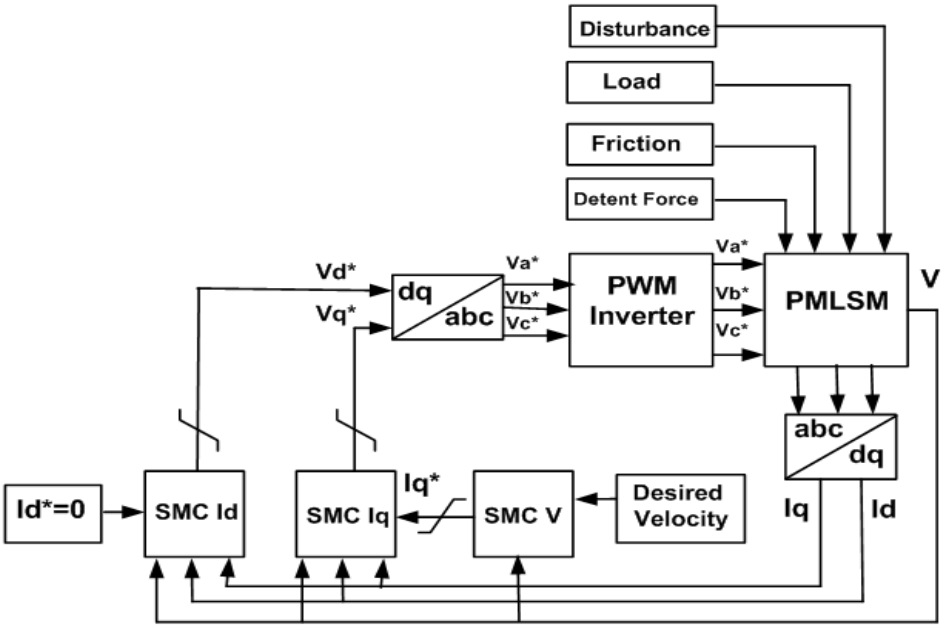

Fig. 2: Schematic diagram of sliding mode controller

Since the aim of this study is to achieve velocity control and to track the reference value in presence of uncertainty and external disturbances, the error vector is defined as follows:

$$E = \begin{bmatrix} i_d - i_d^* & i_q - i_q^* & v - v^* \end{bmatrix}^T = \begin{bmatrix} e_1 & e_2 & e_3 \end{bmatrix}^T \quad (18)$$

where i^*_d and i^*_q are reference currents and v^* is the desired velocity.

Sliding surfaces are chosen with respect to the form of plant equations as follow:

$$S_1 = e_1 + k.\int_0^t e_1 dt + e_1(0) \quad (19)$$

$$S_2 = e_2 + n.\int_0^t e_2 dt + e_2(0) \quad (20)$$

$$S_3 = \dot{e}_3 + c.e_3 \quad (21)$$

where k, n and c are positive constants which determine the dynamics of sliding surfaces and converging rate of error vector to zero.

Assuming $V_1 = 0.5S^2_1$ as Lyapanov function, the error vector may converge to zero in limited time and sliding mode is so-called accessible if $\dot{V}_1 = S_1.\dot{S}_1<0$ is satisfied:

$$\begin{aligned} \dot{V}_1 = S_1.\dot{S}_1 = S_1.(-\hat{R}/\hat{L}).i_d + \pi.v.i_q/\tau \\ + V_d/\hat{L} - i_d^* + k.(i_d - i_d^*)) = S_1.(f + U + U^*) \end{aligned} \quad (22)$$

where, $f = -\hat{R}.i_d/\hat{L} + \pi.v.i_q/\tau$; $U = V_d/\hat{L}$; $U^* = -i^*_d + k.(i_d - i^*_d)$.

Taking uncertainty into account, the final equation is as follows:

$$\begin{aligned} U_d &= L.(-U^* - \Delta U') \\ &= L.(\dot{i}_d^* - k.i_d + k.i_d^* - (F^U + \beta), Sat(S_1)) \end{aligned} \quad (23)$$

where $|f| \le F^U$ and $\Delta U' = (F^U + \beta)Sat(S_1)$

Similarly, for the reference voltage of q-axis:

$$\begin{aligned} V_q = \pi.\hat{L}.v.i_d/\tau + (\hat{R} - n.\hat{L}).i_q \\ + \pi.\hat{\lambda}_{PM}.v/\tau + n.L.i_q^* + L.\dot{i}_q^* - \gamma.Sat(S_2) \end{aligned} \quad (24)$$

$$\begin{aligned} U_q &= L.(-U^* - \Delta U') \\ &= L.(\dot{i}_q^* - n.i_q + n.i_q^* - (F^U + \gamma).Sat(S_2)) \end{aligned} \quad (25)$$

According to the chosen sliding surface in (21) and after differentiation, relation (26) is achieved:

$$\begin{aligned} \dot{S}_3 &= \ddot{e}_3 + c.\dot{e}_3 = f + B_m.U + g - \dot{v}_m + c.\dot{e}_3 \\ &= U^* + \Delta U^* + B_m.U \end{aligned} \quad (26)$$

Notice that the reference current of q-axis is considered as output of controller (U = i^*_q). Taking uncertainty into account, the final control signal is as follows:

$$U_v = -(U^* + \Delta U')/B_L \quad (27)$$

where, $\Delta U' = (F^U + G^U + \alpha)$. Sat (S_3) and after mathematical replacement in (27) the following equation may be achieved:

$$\begin{aligned} i_q^* &= U_v \\ &= [\dot{v}^* - c.(v - v^*) - (F^U + G^U + \alpha).Sat(S_3)]/B_L \end{aligned} \quad (28)$$

Based on Fig. 2 and the state vector as (29), it can be said that the two controllers of q-axis loop actually play a cooperative role together to track the desired velocity by applying the control signal through the reference current of q-axis:

$$\overline{X} = \begin{bmatrix} i_d & i_q & v \end{bmatrix}^T \quad (29)$$

Duty of the current control loop on d-axis is to keep the value of current to zero ($i_d = 0$). Equations of the PMLSM are such that the interaction between state variables cannot be ignored. The most important reason is that the velocity is related to all three equations. As a result, the velocity is an important input for all controllers at any instant.

PI controller: In this section in order to have an evaluation criterion for the performance of the designed sliding mode controller, a proportional integral controller is designed. The SMC blocks in simulation environment are replaced with the classic PI controllers. The most important controller among the three PI blocks is the one which produces i^*_q using desired value of velocity. In other words, the two other PI blocks have less effect on tracking process. Therefore, the unimportant PI controllers can be tuned using decoupling method and calculating corresponding transfer function. In this method, axis voltages are decoupled and become independent of each other by means of feed forward terms as follows:

$$u_{dcpl-d} = -\pi.v.\phi_q/\tau = -\pi.v.L_q.i_q/\tau \quad (30)$$

$$u_{dcpl-q} = \pi.v.\phi_d/\tau = \pi.v.(L_d.i_d + \lambda_{PM})/\tau \quad (31)$$

Table 1: PSO parameters

Number of particles	50
Iteration	150
Learning factors	$C_1 = C_2 = 1.5$
Inertia weight	$0.1 < W < 0.6$

Table 2: Specifications of PMLSM

Parameter	Value
Armature resistance (per phase)	2.4 Ω
Inductance (per phase)	0.0233 H
Equivalent flux of PM	0.5171 Wb
Pole pairs	2
Pole pitch	0.0305 m
Velocity	0.3 m/sec
Inverter voltage (DC)	250 V
Mass of mover	2.5 kg
Load	73 N
Power	54 W
Continuous current	1.6 A
Peak current	4.8 A

Table 3: Parameters with uncertainty and boundary values

Parameter	Max.	Min.
Armature resistance (per phase)	5 Ohm	1 Ohm
Inductance (per phase)	0.025 H	0.020 H
Equivalent flux of PM	0.52 Wb	0.50 Wb

Min.: Minimum; Max.: Maximum

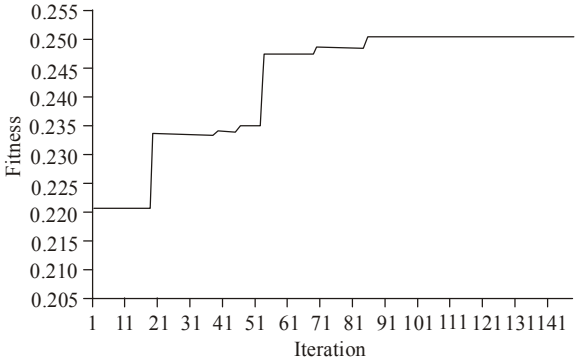

Fig. 3: Improvement of fitness function

The transfer function calculated for d-axis is expressed by the following relation:

$$G_d(s) = i_d(s)/i_d^*(s) = (K_{Pd}.s + K_{Id})/(L_d.s^2 + (K_{Pd}.s + R).s + K_{Id}) \quad (32)$$

Using this function and choosing the cut-off frequency with regard to the desired bandwidth, optimal coefficients can be $K_{pd} = L_d.\omega_c$ and $K_{Id} = R.\omega_c$. Similarly, for q-axis there are $K_{pq} = L_q.\omega_c$ and $K_{Iq} = R.\omega_c$.

Apparently, due to importance of the last PI block as mentioned before, an evolutionary algorithm is necessary to optimize the controller coefficients. Therefore, an optimization procedure based on PSO algorithm is carried out with the given parameters in Table 1. The corresponding curve of fitness function improvement is shown in Fig. 3.

Next, simulations for both SMC and PI velocity control in MATLAB SIMULINK® environment are developed. Specifications of PMLSM are listed in Table 2 (Liu *et al*., 2007). Boundary values of uncertain parameters are also provided in Table 3.

Generally, robustness of controller can be evaluated by applying external disturbances such as detent force, nonlinear friction and unpredicted load (F_d) altogether and also taking parametric uncertainties into account. Figure 4 illustrates simulation results for both PI-PSO and SMC in response to a trapezoidal velocity profile. Afterwards, Fig. 5 depicts the results of simulations performed for the step desired value of velocity where a sudden disturbance is applied in the form of a 146 N force. Added disturbance at t = 0.04 is equal to 200% increase in force. Based on the simulation results it is vivid that the sliding mode control is successful on tracking of desired velocity. PI-PSO controller due to dilatory transient mode does not have ability to follow velocity profiles with rapid changes. In case that the desired velocity is step-like, the reference current of q-axis may reach the maximum

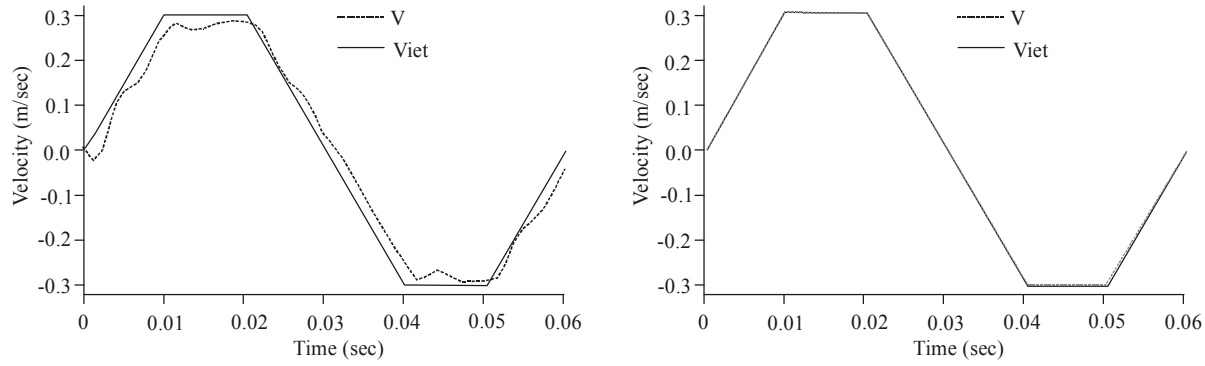

Fig. 4: Trapezoid velocity command; (a): PI-PSO; (b): SMC

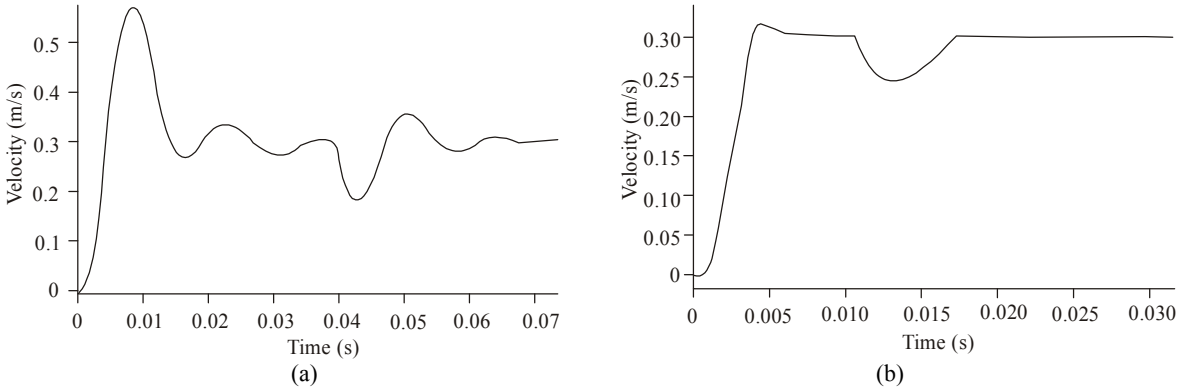

Fig. 5: Step response of velocity with 200% load increase; (a): PI-PSO; (b): SMC

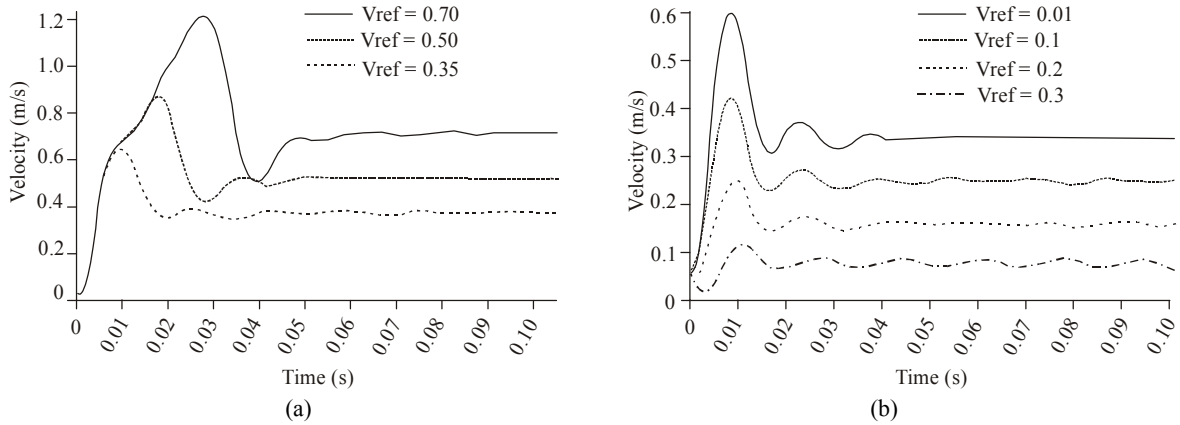

Fig. 6: Step responses of PI-PSO with different reference velocities; (a): Lower than nominal; (b): Higher than nominal

tolerable limit on transient state, as a result, the tracking process would be more sluggish.

Encountering sudden load disturbances, provided that the reference current of q-axis does not enter to the saturation level, the SMC performance is very successful. In case that the perturbation is applied at two hundred per cent, SMC performance is pretty better than PI-PSO in accordance with the expectation.

THE PROPOSED ROBUST ADAPTIVE SLIDING MODE CONTROLLER

Regarding the wide variety of applications for PMLSM, it is required to control velocity in a wide range. Even for a motor with special application the operating velocity may vary from high to about zero and even reverse. On the other hand, effect of disturbance, detent force and nonlinear friction at low velocities and no-load state is more evident. Therefore, the ability to control about zero velocity is more important and reveals merit of controller.

Initially, the reference velocity is changed into very high and very low values; hence, the performances of both PI and sliding mode controller are evaluated and compared. Based on Table 2, the nominal reference velocity is 0.3 m/sec. Subsequently, Fig. 6 depicts simulation results for different reference velocities lower and upper than nominal value for PI-PSO controller. Similarly the results for sliding mode controller are depicted in Fig. 7.

Regarding the illustrated results, PI controller does not have a satisfying performance encountering with different reference velocities. However, sliding mode controller also has tracking error due to the parameters of SMC which are set for the nominal velocity.

This section tries to expand and generalize the structure of classic SMC to achieve an acceptable tracking performance over a wider range. By changing the reference velocity in the range above the nominal value, gradually steady state error and undesirable oscillations appear. The coefficients of sliding surface and switching function could be changed to overcome this problem and may lead to improvement in the tracking issue. In the same way, it is possible to tune the SMC for very low velocities.

The most effective parameters in SMC are coefficients in (4.13). To enhance the behavior of SMC at higher and lower velocities, it is needed to change c and choose a new sliding surface to escape the steady and dynamic errors. Utilizing different coefficients to form a lookup table, an adaptive mechanism for modifying and automatic tuning of SMC parameters is designed. Notable point is how to segment velocity ranges and to choose thickness of bands. Considering

the results obtained in previous section, the thickness of velocity bands is chosen equal to 0.1 m/sec. This means that an increase or decrease in the reference velocity which exceeds the current band, immediately leads to change the coefficients of SMC. As a typical scheme, nominal velocity is assumed 0.3 m/sec and four adaptive bands are predicted up to 0.7 m/sec. On the other hand, at low velocities more precision is required because of both the nonlinear behavior of friction and ripple force Therefore, the lower velocity is divided into narrow bands; i.e., the thickness of bands about zero velocity is chosen about 0.1 m/sec. As reference

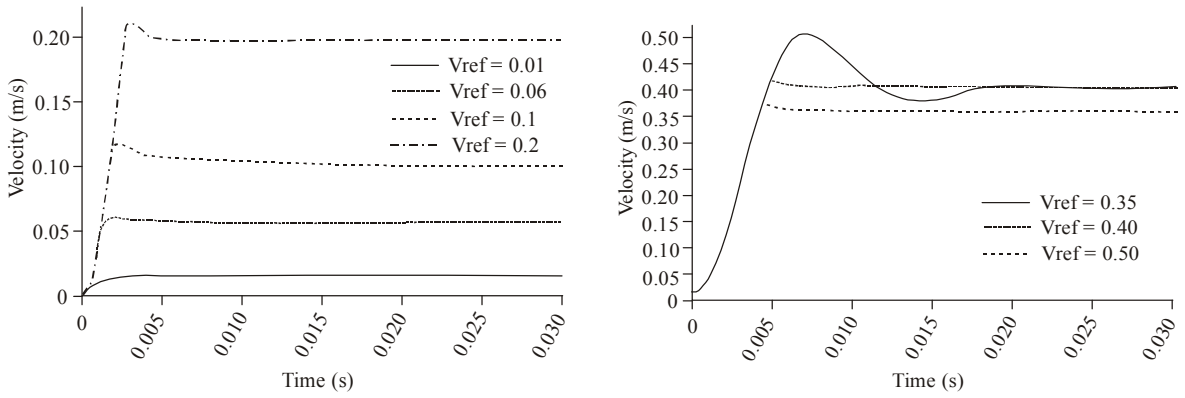

(a) (b)

Fig. 7: Step responses of SMC with different reference velocities; (a): Lower than nominal; (b): Higher than nominal

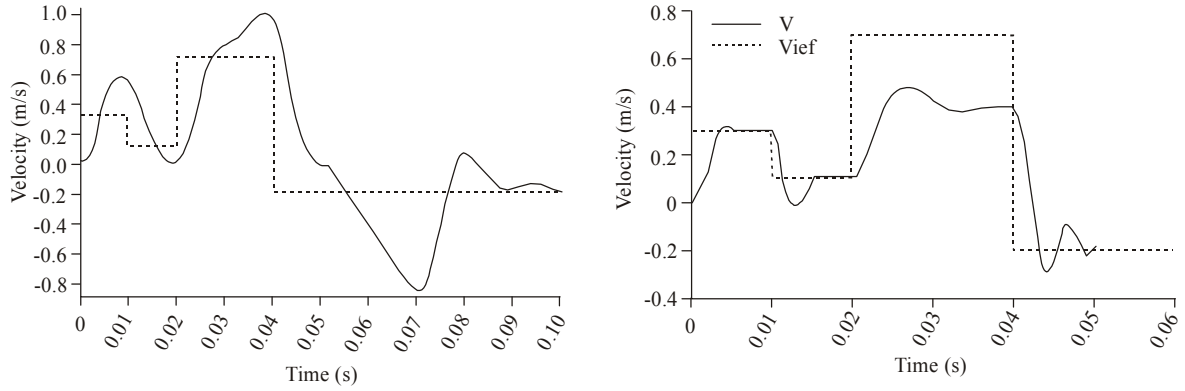

(a) (b)

Fig. 8: Velocity with time varying reference command; (a): PI-PSO; (b): SMC

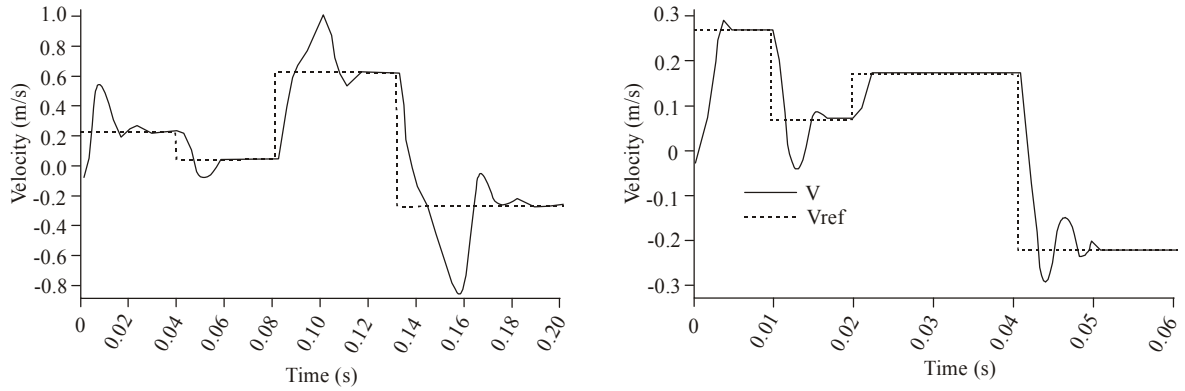

(a) (b)

Fig. 9: Velocity with a soft time varying reference command; (a): PI-PSO; (b): SMC

velocity decreases from 0.15 m/sec to 0, impact of α decreases gradually and c becomes more important. Undoubtedly, tuning of SMC for low velocity is quite more difficult rather than high velocity. However, coefficients of SMC are easier to set compared with PI controller. In fact, the structure of SMC unlike PI is less dependent on these coefficients. Hence, there is no need for optimization algorithm.

Consequently, Fig. 8 shows simulation results of both PI-PSO and adaptive SMC in response to a time varying velocity profile. Vividly, reference velocity has severe and rapid changes which compel the reference current of q-axis to jump to the maximum limits. Therefore, the ability of controlling and tracking the desired velocity might be disrupted. Since the transient state of PI controller is too slow, it cannot follow reference velocities with rapid jumps. Hence, another reference velocity which is softer and smoother is applied to both PI-PSO and sliding mode controller (Fig. 9). Obviously, if a slower reference value is applied to PI controller, the result can be quite satisfying regardless of transient state. Indeed, here the applied reference velocity is still fast but salient jumps are eliminated. Considering the recent figures, it can be concluded that the reference current of q-axis has not exceeded the limits; therefore, tracking of desired velocity profile is perform well.

CONCLUSION

Non-idealities such as detent force, parameter uncertainty, unpredicted disturbance and nonlinear friction were taken into account to obtain a comprehensive nonlinear model of the PMLSM. By considering a variable velocity profile in a wide range in addition to the above mentioned uncertainties and disturbances, an adaptive robust variable structure speed controller was suggested for desired velocity control of a PMLSM. The proposed method is based on robust SMC in combination with an adaptive mechanism for a wide range of velocity.

As the SMC is high gain, the main drawback is the saturation of control signal. Therefore, if the toleration limits of plant are not extensive, tracking performance is deteriorated. Moreover, if the reference velocity profile does not include severe changes, reference current of q-axis can be remained in the scope of permissible value and PMLSM tracks desired velocity ideally.

ACKNOWLEDGMENT

Special thanks are dedicated to the Center of Research and Technology at the University of Isfahan for their full support. Valuable comments from Dr. S. Mohammad Madani indeed helped to significantly improve and enhance the contents of this research. The authors would really appreciate his comprehensive attentions.

REFERENCES

Bernardes, T., V. Foletto Montagner, H.A. Grundling and H. Pinheiro, 2014. Discrete-time sliding mode observer for sensorless vector control of permanent magnet synchronous machine. IEEE T. Ind. Electron., 61(4): 1679-1691.

Ghaebi Panah, P., A. Shafiei and R. Sharifian, 2010. An improved variable structure design for velocity control of a permanent magnet linear synchronous motor. Proceeding of IEEE International Conference on Power Electronics Electrical Drives Automation and Motion, pp: 1231-1236.

Ghaebi Panah, P., M. Ataei and A. Shafiei, 2011a. An adaptive fuzzy sliding mode control of a permanent magnet linear synchronous motor for an inimical command velocity profile. Proceeding of IEEE International Conference on System Engineering and Technology, pp: 41-46.

Ghaebi Panah, P., A. Shafiei, A. Parsa Pour and B. Mirzaeian Dehkordi, 2011b. Velocity control of a PMLSM using a brain emotional learning based intelligent control strategy. Proceeding of IEEE International Conference on System Engineering and Technology, pp: 47-52.

Hong, J., D. Pan and Z. Zong, 2013. Comparison of the two current predictive-control methods for a segment-winding permanent-magnet linear synchronous motor. IEEE T. Plasma Sci., 41(5): 1167-1173.

Hwang, C.C., P.L. Li and C.T. Liu, 2012. Optimal design of a permanent magnet linear synchronous motor with low cogging force. IEEE T. Magn., 48(2): 1039-1042.

Inoue, M. and K. Sato, 2000. An approach to a suitable stator length for minimizing the detent force of permanent magnet linear synchronous motors. IEEE T. Magn., 36: 1890-1893.

Jia, Z., P.J. Barre and P. Degobert, 2003. Modeling and thrust control of PMLSM using principle of local energy. Proceeding of International Conference on Electrical Machines and Systems, pp: 26-30.

Kim, S., Y. Zhu, S. Lee, S. Saha and Y. Cho, 2014. Electromagnetic normal force characteristics of a permanent magnet linear synchronous motor with double primary side. IEEE T. Magn., 50(1): 1-4.

Kung, Y.S., 2008. Design and implementation of a high-performance PMLSM drives using DSP chip. IEEE T. Ind. Electron., 55: 1341-1351.

Lee, S., S. Kim, S. Saha, Y. Zhu and Y. Cho, 2014. Optimal structure design for minimizing detent force of PMLSM for a ropeless elevator. IEEE T. Magn., 50(1): 1-4.

Lin, F.J., P.H. Chou, Y.C. Hung and W.M. Wang, 2010. Field-programmable gate array-based functional link radial basis function network control for permanent magnet linear synchronous motor servo drive system. IET Electr. Power App., 4(5): 357-372.

Lin, F.J., H.J. Hsieh, P.H. Chou and Y.S. Lin, 2011. Digital signal processor-based cross-coupled synchronous control of dual linear motors via functional link radial basis function network. IET Control Theory A., 5(4): 552-564.

Liu, Y., B. Tan and X. Zhang, 2007. Position accuracy improvement of PMLSM system based on artificial immune algorithm. Proceeding of International Conference on Mechatronics and Automation, pp: 3679-3683.

Liyi, L., H. Junjie, W. Hongxing, Z. Zhe and L. Xiaopeng, 2008. Adaptive back-stepping control for the sectioned permanent magnetic linear synchronous motor in vehicle transportation system. Proceeding of Vehicle Power and Propulsion Conference, pp: 1-5.

Lu, H.C. and M.H. Chang, 2009. Automatic generation fuzzy neural network controller with supervisory control for permanent magnet linear synchronous motor. Proceeding of 4th IEEE Conference on Industrial Electronics and Applications, pp: 3124-3129.

Orbak, A.Y., 2003. Modeling and full state feedback adaptive control of a two dimensional linear motor. Proceeding of Control Applications Conference, pp: 791-796.

Ouassaid, M. and M.C. Rkaoui, 2005. Nonlinear torque control for PMSM: A lyapunov technique approach. IEEE T. Eng. Comput. Technol., 6: 118-121.

Rivera, D.J., A. Navarrete, M.A. Meza, A.G. Loukianov and J. Canedo, 2014. Digital sliding-mode sensorless control for surface-mounted PMSM. IEEE T. Ind. Inform., 10(1): 137-151.

Seong, L.H. and M. Tomizuka, 1996. Robust motion controller design for high-accuracy positioning systems. IEEE T. Ind. Electron., 43: 48-55.

Shin, J., R. Watanabe, T. Koseki and H. Kim, 2014. Transverse-flux-type cylindrical linear synchronous motor using generic armature cores for rotary machinery. IEEE T. Ind. Electron., 61(8): 4346-4355.

Tavana, N.R., A. Shoulaie and V. Dinavahi, 2012. Analytical modeling and design optimization of linear synchronous motor with stair-step-shaped magnetic poles for electromagnetic launch applications. IEEE T. Plasma Sci., 40(2): 519-527.

Van Den Braembussche, P., J. Swevers and H. Van Brussel, 1996. Accurate tracking control of linear synchronous motor machine tool axes. J. Sci. Mechatron., 6: 507-521.

Xie, Q., 2008. Modeling and control of linear motor feed drives for grinding machines. Ph.D. Thesis, George W. Woodruff School of Mechanical Engineering, Georgia Institute of Technology.

Yang, J., G. He and J. Cui, 2006. Analysis of PMLSM direct thrust control system based on sliding mode variable structure. Proceeding of CES/IEEE 5th International Power Electronics and Motion Control Conference, pp: 1-5.

Zhao, Y., Q. Wang, J. Xu and C. Wang, 2007. A fuzzy sliding mode control based on model reference adaptive control for permanent magnet synchronous linear motor. Proceeding of IEEE Conference on Industrial Electronics and Applications, pp: 980-984.